Mathematical Geology, Vol. 36, No. 2, February 2004 (© 2004)

Stochastic Modeling of Variably Saturated Transient Flow in Fractal Porous Media[1]

Luis Guarracino[2] and Juan E. Santos[2,3]

This work presents the application of a Monte Carlo simulation method to perform an statistical analysis of transient variably saturated flow in an hypothetical random porous media. For each realization of the stochastic soil parameters entering as coefficients in Richards' flow equation, the pressure head and the flow field are computed using a mixed finite element procedure for the spatial discretization combined with a backward Euler and a modified Picard iteration in time. The hybridization of the mixed method provides a novel way for evaluating hydraulic conductivity on interelement boundaries. The proposed methodology can handle both large variability and fractal structure in the hydraulic parameters. The saturated conductivity K_s and the shape parameter α_{vg} in the van Genuchten model are treated as stochastic fractal functions known as fractional Brownian motion (fBm) or fractional Gaussian noise (fGn). The statistical moments of the pressure head, water content, and flow components are obtained by averaging realizations of the fractal parameters in Monte Carlo fashion. A numerical example showing the application of the proposed methodology to characterize groundwater flow in highly heterogeneous soils is presented.

KEY WORDS: unsteady unsaturated flow, finite elements, heterogeneous soils.

INTRODUCTION

Groundwater flow and contaminant transport are significantly influenced by heterogeneous soil properties. At field scale, soils parameter distributions are subject to uncertainty due the high degree of spatial variability and the relatively small number of subsurface observations. For this reason, in the last two decades, the theory of stochastic processes has been used to study the effect of spatial variability in water flow and solute transport.

One of the most widely used methods to solve stochastic flow equations is based on Monte Carlo simulation. In the Monte Carlo approach a set of realizations of the stochastic soil parameters with a given statistical characterization is

[1]Received 20 September 2001; accepted 4 June 2003.

[2]CONICET, Facultad de Ciencias Astronómicas y Geofísicas, Universidad Nacional de La Plata, La Plata 1900, Argentina; e-mail: luisg@fcaglp.fcaglp.unlp.edu.ar; santos@fcaglp.fcaglp.unlp.edu.ar

[3]Department of Mathematics, Purdue University, West Lafayette, Indiana 47907-1395; e-mail: santos@math.purdue.edu

synthetically generated. For each realization a deterministic flow problem is solved using a numerical method. After a large number of realizations the statistical moments of the computed variables are calculated. The Monte Carlo method can handle complex geometries and deal with extremely large variability in stochastic parameters, avoiding the commons limitations of the perturbation approach. Its main disadvantage is associated with the computational cost. Analysis of water flow and solute transport in highly heterogeneous aquifers were presented by Ünlü, Nielsen, and Biggar (1990), Hassan, Cushman, and Delleur (1998), Salandin and Fiorotto (1998), Naff, Haley, and Sudicky (1998), and Harter and Yeh (1998).

The objective of this work is to present a numerical procedure to simulate transient groundwater flow in heterogeneous fractal porous media. Field measurements shows that the soil parameters have a high degree of spatial variability and exhibit long range correlations that are better described by stochastic fractals instead of the classical Gaussian processes. Consequently a Monte Carlo simulation method is needed to tackle this problem. A robust numerical procedure that be able to handle large discontinuities in the coefficients of the flow equations at the grid level is also required. The use of a mixed finite element method for the spatial discretization of the flow equations is especially suitable for the latter purpose.

Groundwater flow in variably saturated soils is assumed to be described by Richards equation (Richards, 1931), a highly nonlinear parabolic equation. Standard finite element methods for solving Richards equation have been used by Celia, Bouloutas, and Zarba (1990), Allen and Murphy (1985) among others. Recently, mixed finite element methods have been employed to simulate groundwater flow both for saturated (Beckie, Wood, and Aldama, 1993; Mosé and others, 1994) and unsaturated conditions (Bergamaschi and Putti, 1999; Chounet and others, 1999).

In this paper Richards equation is solved using a hybridized mixed finite element procedure. Because of the high nonlinearity of the equation, quadrature rules for computing integrals are required. When a trapezoidal quadrature is used, the nonlinear coefficients in Richards equation need to be evaluated on interelement boundaries. The hybridization of the mixed finite element introduces a new variable (a Lagrange multiplier) associated with the values of the potential on interelement boundaries. Using the Lagrange multipliers to evaluate the nonlinear coefficients provided us with a natural and numerically efficient procedure that allows to handle the large discontinuities and high spatial variability related to the fractal structure of the hydraulic parameters, avoiding the usual approach of performing averages or the common assumption that the nonlinear coefficients are constant over the elements.

To solve Richards equation, constitutive relationships of hydraulic conductivity (K) and water content (θ) versus pressure head (h) must be specified. One of the models frequently employed in numerical simulation of water flow is the van Genuchten model (van Genuchten, 1980); which involve the saturated hydraulic conductivity (K_s) and a shape parameter α_{vg}. At field scale, these parameters

show a high degree of spatial variability and need to be characterized using a statistical approach (Russo and Bouton, 1992; Russo, Russo, and Laufer, 1997). Neuman (1994), Kemblowski and Chang (1993), and Moltz and Boman (1995) had reported evidences of fractal structure in saturated hydraulic conductivity (K_s) distributions. In those works K_s distributions are described employing stochastic fractal functions, such as fractional Brownian motion (fBm) or fractional Gaussian noise (fGn).

To illustrate the use of the proposed stochastic model we designed an infiltration test in a hypothetical random porous media where both K_s and α_{vg} obey either fBm or fGn statistics. More specifically, a set of realizations of the stochastic parameters is synthetically generated using a fractal generator based on a spectral method. For each realization a deterministic problem associated with Richards equation is solved using a hybridized mixed finite element method for the spatial discretization combined with a backward Euler and a Picard iteration for the time discretization. After a large number of realizations the statistical moments of the pressure head, water content, and flow vector are calculated. To stop the Monte Carlo method, a criteria based on the stabilization of a global measure of the variances of the computed variables is proposed.

THE DIFFERENTIAL MODEL FOR VARIABLY SATURATED FLOW

Let Ω be a bounded porous domain with boundary $\partial\Omega$. For the spatial Cartesian coordinates $\mathbf{x} = (x, y, z)$ let $\theta = \theta(\mathbf{x})$, $h = h(\mathbf{x})$, and $\mathbf{q} = \mathbf{q}(\mathbf{x})$ denote the water content, the pressure head, and the flow vector, respectively. It will be assumed that water flow in Ω is governed by Richards equation (Richards, 1931) stated in the form

$$\frac{\partial\theta(h)}{\partial t} + \nabla\cdot\mathbf{q} = 0, \quad \mathbf{x}\in\Omega, \tag{1a}$$

$$\mathbf{q} = -K(h)\nabla(h+z), \quad \mathbf{x}\in\Omega, \tag{1b}$$

with boundary conditions

$$\mathbf{q}\cdot\boldsymbol{\nu} = q^*, \quad \mathbf{x}\in\Gamma^N, \tag{2a}$$

$$h = h^*, \quad \mathbf{x}\in\Gamma^D, \tag{2b}$$

and initial condition $h = h^0$, $\mathbf{x}\in\Omega$. In the above equations t is the time variable and the z-axis is considered to be positive upwards. In (2a) $\boldsymbol{\nu}$ denotes the unit outer normal to $\partial\Omega$; Γ^D and Γ^N denote respectively the part of the boundary where the pressure head values h^* and the normal component of the flow q^* are being specified, with $\partial\Omega = \Gamma^D \cup \Gamma^N$, $\Gamma^D \cap \Gamma^N = \emptyset$.

To solve the differential problem (1)–(2) we consider the van Genutchen model (van Genutchen, 1980):

$$\theta(h) = \begin{cases} \dfrac{\theta_s - \theta_r}{[1 + (\alpha_{vg}|h|)^n]^m} + \theta_r, & \text{for } h < 0 \\ \theta_s & \text{for } h \geq 0 \end{cases} \tag{3}$$

$$K(h) = \begin{cases} K_s \dfrac{\{1 - (\alpha_{vg}|h|)^{n-1}[1 + (\alpha_{vg}|h|)^n]^{-m}\}^2}{[1 + (\alpha_{vg}|h|)^n]^{m/2}} & \text{for } h < 0 \\ K_s & \text{for } h \geq 0 \end{cases} \tag{4}$$

where θ_r and θ_s are the residual and saturated water contents, respectively; n and α_{vg} are shape parameters; and m is given by the relation $m = 1 - 1/n$.

The first step to approximate the solution of the flow equations is to discretize in time (1) using a backward Euler method coupled with a modified Picard iteration scheme (Celia, Bouloutas, and Zarba, 1990) as follows:

$$\frac{\theta^{n+1,i} - \theta^n}{\Delta t^n} + \frac{C^{n+1,i}}{\Delta t^n}\delta h^{i+1} + \nabla \cdot \mathbf{q}^{n+1,i+1} = 0, \quad \mathbf{x} \in \Omega, \tag{5a}$$

$$\frac{\mathbf{q}^{n+1,i+1}}{K^{n+1,i}} + \nabla(h^{n+1,i} + \delta h^{i+1} + z) = 0, \quad \mathbf{x} \in \Omega, \tag{5b}$$

where the superscripts n and i denote time and iteration level, respectively; $\Delta t^n = t^{n+1} - t^n$ is the time step; $\delta h^{i+1} = h^{n+1,i+1} - h^{n+1,i}$; $\theta^{n+1,i} = \theta(h^{n+1,i})$; $C^{n+1,i} = (\frac{\partial \theta}{\partial h})^{n+1,i}$; and $K^{n+1,i} = K(h^{n+1,i})$.

A HYBRIDIZED MIXED FINITE ELEMENT PROCEDURE

Let us consider the solution of the flow equations (5) using a hybridized mixed finite element method for the case in which the domain Ω is a rectangle. Let $\mathcal{T}^{\tilde{h}}$ be a nonoverlapping partition of Ω into rectangles Ω_j, $j = 1, \ldots, n_j$, of diameter bounded by $\tilde{h}$. Also, set $\Gamma_{jk} = \partial\Omega_j \cap \partial\Omega_k$, $\Gamma_j = \partial\Omega_j \cap \partial\Omega$.

For $l \geq 0$ let V^l and W^l be the Raviart–Thomas–Nedelec (Douglas and Roberts, 1985; Nedelec, 1980; Raviart and Thomas, 1977) mixed finite element space of index l associated with $\mathcal{T}^{\tilde{h}}$, i.e.,

$$V^l = \{\mathbf{v} \in H(\text{div}, \Omega) : \mathbf{v}|_{\Omega_j} \in P_{l+1,l} \times P_{l,l+1}\},$$

$$V_0^l = \{\mathbf{v} \in V^l \text{ and } \mathbf{v} \cdot \boldsymbol{\nu} = 0 \text{ on } \Gamma^N\},$$

$$W^l = \{\psi \in L^2(\Omega) : \psi|_{\Omega_j} \in P_l\},$$

where P_m denote the polynomials of total degree not greater than m and $P_{m,n}$ denotes the polynomials of degree not greater than m in the x-variable and not

greater than n in the z-variable. In order that elements $\mathbf{v} \in V^l$ be in $H(\text{div}, \Omega)$ their normal components must be continuous across the interelement boundaries Γ_{jk}. The algebraic problem associated to the mixed finite element procedure for the approximate solution of (5) consists of the solution of a linear system of equations for the coefficients of the expansion of the flow vector and pressure head in a basis of $V_0^l \times W^l$. Following Arnold and Brezzi (1985), we will simplify the algebraic form associated with the mixed method by eliminating the constraint imposing the continuity of the normal components of the flow vector across the interior boundaries and enforcing the required continuity instead using a Lagrange multiplier. Thus we introduce a space of Lagrange multipliers Λ^l which elements λ are associated with the potential $h + z$ at the interelement boundaries Γ_{jk}. Let

$$\Lambda^l = \{\lambda : \lambda|_{\Gamma_{jk}} = \lambda_{jk} \in P_l(\Gamma_{jk})\},$$
$$V_{-1}^l = \{\mathbf{v} \in L^2(\Omega) : \mathbf{v}|_{\Omega_j} \in P_{l+1,l} \times P_{l,l+1}\},$$
$$V_{0,-1}^l = \left\{\mathbf{v} \in V_{-1}^l \text{ and } \mathbf{v} \cdot \boldsymbol{\nu} = 0 \text{ on } \Gamma^N\right\}.$$

Next, to obtain a hybridized form of the mixed method we multiply (5a) by $\psi \in W^l$ and integrate over Ω. Also, we multiply (5b) by $\mathbf{v} \in V_{0,-1}^l$ and integrate over Ω, using integration by parts at the element level in the second term in the left-hand side of (5b) and the fact that the Lagrange multipliers are associated with the potential $h + z$ on Γ_{jk}. Note that we cannot use integration by parts globally in Ω because functions in $V_{0,-1}^l$ do not have divergence defined globally in $L^2(\Omega)$.

Thus, if $\mathbf{Q}$ and H denote the discrete water flow and pressure head, the hybridized mixed finite element procedure is defined in the following fashion: Let $(\mathbf{Q}^n, H^n, \lambda^n) \in V_{-1}^l \times W^l \times \Lambda^l$ be given and such that $(\mathbf{Q}^n, H^n)$ satisfies (2). Then, given $(\mathbf{Q}^{n+1,0}, H^{n+1,0}, \lambda^{n+1,0}) \in V_{-1}^l \times W^l \times \Lambda^l$, find $(\mathbf{Q}^{n+1,i+1}, H^{n+1,i+1}, \lambda^{n+1,i+1}) \in V_{-1}^l \times W^l \times \Lambda^l$ such that

$$\int_\Omega \left[\frac{\theta^{n+1,i} - \theta^n}{\Delta t^n} + \frac{C^{n+1,i}}{\Delta t^n}\delta H^{i+1}\right]\psi \, d\Omega + \sum_j \int_{\Omega_j} \nabla \cdot \mathbf{Q}^{n+1,i+1}\psi \, d\Omega = 0, \psi \in W^l, \tag{6a}$$

$$\int_\Omega \frac{\mathbf{Q}^{n+1,i+1}}{K^{n+1,i}} \cdot \mathbf{v} \, d\Omega - \sum_j \int_{\Omega_j} (\delta H^{i+1} + H^{n+1,i} + z)\nabla \cdot \mathbf{v} \, d\Omega + \int_{\Gamma^D} (h^* + z)\mathbf{v} \cdot \boldsymbol{\nu} \, d\sigma + \sum_{jk} \int_{\Gamma_{jk}} \lambda_{jk}^{n+1,i+1}\mathbf{v} \cdot \boldsymbol{\nu} \, d\sigma = 0, \quad \mathbf{v} \in V_{0,-1}^l, \tag{6b}$$

$$\mathbf{Q}^{n+1,i+1} \cdot \boldsymbol{\nu} = Q^*, \quad \mathbf{x} \in \Gamma^N, \tag{6c}$$

$$\sum_{jk} \int_{\Gamma_{jk}} \mu \mathbf{Q}^{n+1,i+1} \cdot \boldsymbol{\nu}\, d\sigma = 0, \quad \mu \in \Lambda^l. \tag{6d}$$

Note that Equation (6d) is equivalent to the condition that $\mathbf{Q}^{n+1,i+1} \in H(\text{div}, \Omega)$. In (6c) Q^* is an approximation to q^* defined locally on Γ^N as $Q^*|_{\Gamma_j} = Q_j^*$ for $\Gamma_j \subset \Gamma^N$, where Q_j^* is determined by the relation $\langle Q_j^* - q^*, \varphi \rangle_{\Gamma_j} = 0$, $\varphi \in P_l(\Omega_j)$.

Set $h^{n+1} \equiv h^{n+1,\infty}$, with $h^{n+1,\infty}$ denoting the value of the pressure head after convergence of the Picard iteration has been achieved for a prescribed tolerance, and define $\mathbf{q}^{n+1}$, H^{n+1}, $\mathbf{Q}^{n+1}$ in a similar fashion. Then using the fact that a backward Euler scheme is first order correct in time, the results given in Douglas and Roberts (1985) imply that

$$\|H^{n+1} - h^{n+1}\|_{L^2(\Omega)} \propto \tilde{h}^{l+1} + \max_n \Delta t^n,$$
$$\|\mathbf{Q}^{n+1} - \mathbf{q}^{n+1}\|_{L^2(\Omega)} \propto \tilde{h}^{l+1} + \max_n \Delta t^n.$$

The method (6) was implemented for the lowest-order index case $l = 0$. The corresponding degrees of freedom are the values of the pressure head H^{n+1} at the center of the rectangles Ω_j and the values of the normal component of the water flow vector $\mathbf{Q}^{n+1}$ and the Lagrange multipliers λ^{n+1} at the mid points of the sides of Ω_j.

To compute the first term in the left-hand side of (6b) we employ the following trapezoidal quadrature rule:

$$\int_{\Omega_j} \frac{Q^{n+1,i+1}}{K^{n+1,i}} \cdot \mathbf{v}\, d\Omega \approx \frac{\text{Area of } \Omega_j}{4} \sum_{k=1}^{4} \frac{\mathbf{Q}^{n+1,i+1}}{K^{n+1,i}} \cdot \mathbf{v}\Big|_{\Gamma_{jk}}, \tag{7}$$

where Γ_{jk}, $k = 1, \ldots, 4$, are the four boundaries of the rectangular element Ω_j. Using this quadrature rule we obtain a linear system for the values of the pressure head H^n at the mid points of the rectangles Ω_j, so that in the case $l = 0$ the procedure (6) may be regarded as a cell-centered finite difference scheme.

Numerical computation of (7) requires the evaluation of the nonlinear function $K(h)$ on the interelement boundaries; as explained in the Introduction section, to obtain accurate values of h we employed the Lagrange multipliers associated with the potential at those boundaries, i.e., on the interior boundary Γ_{jk} we obtained $K^{n+1,i}$ using the rule $K^{n+1,i}|_{\Gamma_{jk}} = K(\lambda_{jk}^{n+1,i} - z)$. This novel way of treating nonlinearities provides a natural approach to treat numerically the nonlinearity of $K(h)$ and its high degree of spatial variability (related to the fractal structure of the hydraulic parameters K_s and α_{vg}) and is more accurate than the assumption of

constancy of $K(h)$ over each element as done in (Bergamaschi and Putti, 1999; Chounet and others, 1999).

Numerical solutions of the proposed algorithm were validated in Guarracino (2001) by comparison with analytical solutions presented by Ross and Parlange (1994) and Strivastava and Yeh (1991), including the calculation of the numerical flux across a discontinuity in $K(h)$. Also a dynamic time step control which significantly improved the CPU efficiency was implemented. The time step is increased or decreased depending of the number of iterations required for the Picard iteration to converge.

GENERATION OF FRACTALS USING THE SPECTRAL METHOD

Following Russo and Bouton (1992) and Russo, Russo, and Laufer (1997) we assume that, for $F = K_s$ or $F = \alpha_{vg}$, $\log F(\mathbf{x}) = <\log F> + f(\mathbf{x})$, where $<>$ denotes the mean value and the fluctuation $f(\mathbf{x})$ is a stochastic process. Further we assume that $f(\mathbf{x})$ is either a fBm or a fGn stochastic process.

The spectral density $S_f(\mathbf{k})$ of a fBm/fGn process $f(\mathbf{x})$ in a finite two-dimensional domain can be express (Hassan, Cushman, and Delleur, 1998; Moltz, Liu, and Szulga, 1997):

$$S_f(\mathbf{k}) = \begin{cases} \dfrac{\sigma_f^2(2-\beta)}{4\pi^2\left(k_{\max}^{2-\beta} - k_{\min}^{2-\beta}\right)|\mathbf{k}|^\beta}, & k_{\max} < |\mathbf{k}| < k_{\min} \\ 0, & \text{elsewhere} \end{cases} \tag{8}$$

where $\mathbf{k}$ is the spatial frequency (wave number), σ_f^2 is the variance of $f(\mathbf{x})$; $k_{\min}$ is a lower frequency cutoff which is determinated by the diameter of Ω; $k_{\max}$ is an upper frequency cutoff proportional to the inverse of the finite element mesh size; and β is a parameter related to the fractal dimension D by the formula

$$\beta = \begin{cases} 8 - 2D & \text{for a fBm,} \\ 6 - 2D & \text{for a fGn.} \end{cases} \tag{9}$$

To generate a fBm or a fGn realization we follow the ideas presented by Hassan, Cushman, and Delleur (1998) and Voss (1988). First a set of uniformly distributed random numbers associated with the center of each cell of the finite element mesh is obtained using a random number generator. Then the fast Fourier transform (FFT) of this set of numbers is taken and the resulting numbers are multiplied by a transfer function proportional to $[S_f(\mathbf{k})]^{1/2}$ in the wave number space. Finally, taking the inverse FFT a set of numbers with the desired spectral density (8) is obtained.

Figure 1 shows normalized 2D realizations of fBm and fGn stochastic processes $f(\mathbf{x})$ in a square domain of side length 10 m for several fractal dimensions D and $\sigma_f^2 = 0.1$, with darker pixels corresponding to higher values of f. As expected, as the fractal dimension D increases we have more heterogeneity in the values of f.

Figure 2 shows the covariance $C_f(\boldsymbol{\tau})$ of the fractal fields $f(x)$ in Figure 1 computed using a discrete form of the formula $C_f(\boldsymbol{\tau}) = \langle (f(\mathbf{x}+\boldsymbol{\tau}) - \langle f \rangle)(f(\mathbf{x}) - \langle f \rangle) \rangle$ and 500 realizations. Both for fBm and fGn distributions the correlation length diminishes as the fractal dimension D increases. In the case of a fGn, when D approaches the value 2.5 the process tends to the classical Gaussian noise characterized by having as covariance a Dirac distribution (Fig. 2(b)).

MONTE CARLO SIMULATIONS OF WATER FLOW

The application of the Monte Carlo simulation method to characterize the transient variably saturated flow consists in solving Richards equation for a large number of realizations of the stochastic processes K_s and α_{vg}. We computed the variance of the pressure head, water content, and the water flow at the cell centers of the finite element mesh and observed that the variance values stabilized after a certain number of realizations. Thus we adopted the criteria of stopping the Monte Carlo simulation when a global measure of the variance of the pressure head, water content, and the water flow over the domain Ω have converged to asymptotic values within a small tolerance. More specifically, for $s = h, \theta, q_x, q_z$ we defined the spatial average of the variance of s as follows:

$$\left\| \sigma_s^{2,m} \right\| = \left[\frac{1}{n_j} \sum_{j=1}^{n_j} \left(\sigma_{s_j}^{2,m} \right)^2 \right]^{1/2}, \tag{10}$$

where $\sigma_{s_j}^{2,m}$ denotes the variance of s computed at the center of the subdomain Ω_j after m-realizations. Thus, setting $\Delta\sigma_s^{2,m} = \|\sigma_s^{2,m} - \sigma_s^{2,m-1}\|$, we consider that the Monte Carlo simulation converges when for a given ϵ sufficiently small we have that

$$\frac{\Delta\sigma_s^{2,m}}{\Delta\sigma_s^{2,4}} \leq \epsilon. \tag{11}$$

Once the convergence has been achieved we proceed to compute the statistical moments of the variables of interest. For the stochastic variable s we computed the mean value $\langle s_j \rangle^N$ and variance $\sigma_{s_j}^{2,N}$ associated with the center of the subdomain Ω_j and the covariance $C_{s_j s_k}^N$ associated with the centers of the subdomains Ω_j and

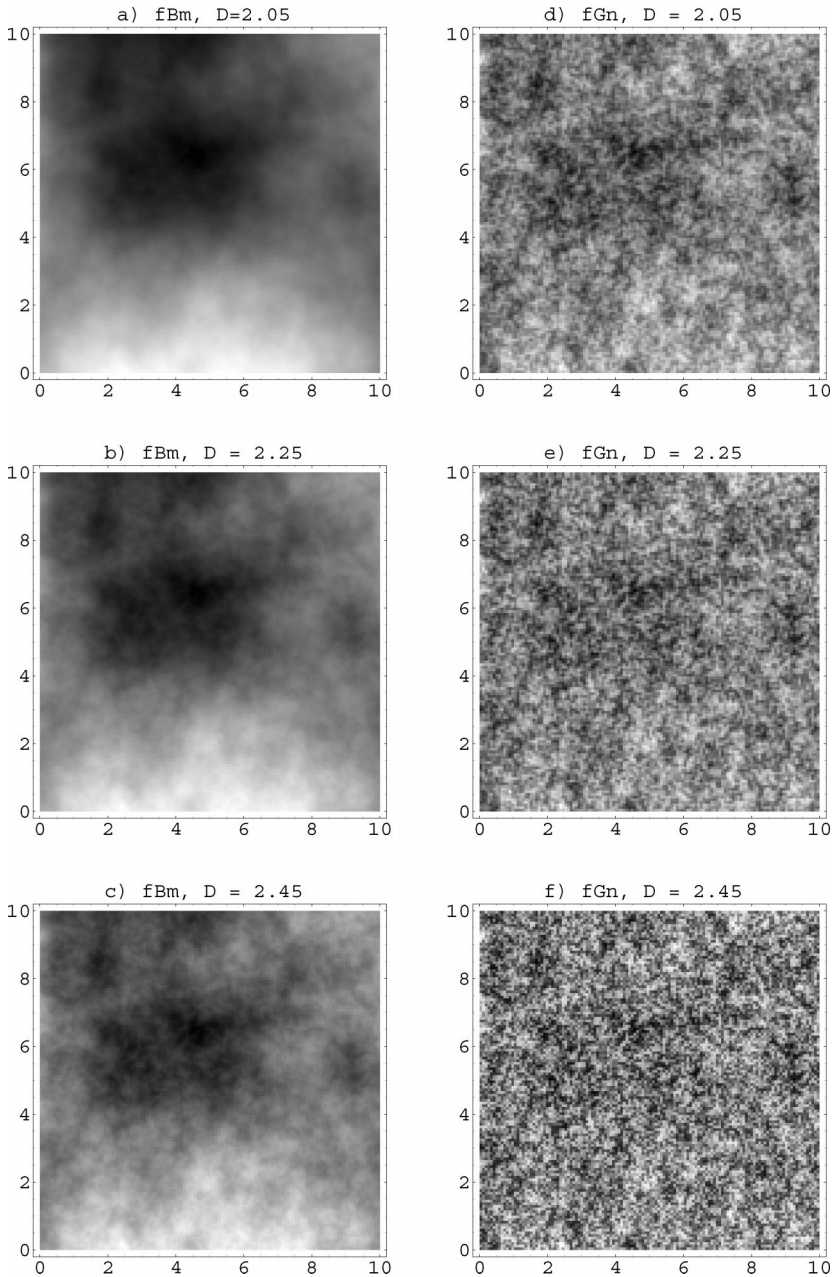

Figure 1. Realizations of fBm distributions for (a) $D = 2.05$, (b) $D = 2.25$, (c) $D = 2.45$ and fGn distributions for (e) $D = 2.05$, (f) $D = 2.25$, (g) $D = 2.45$.

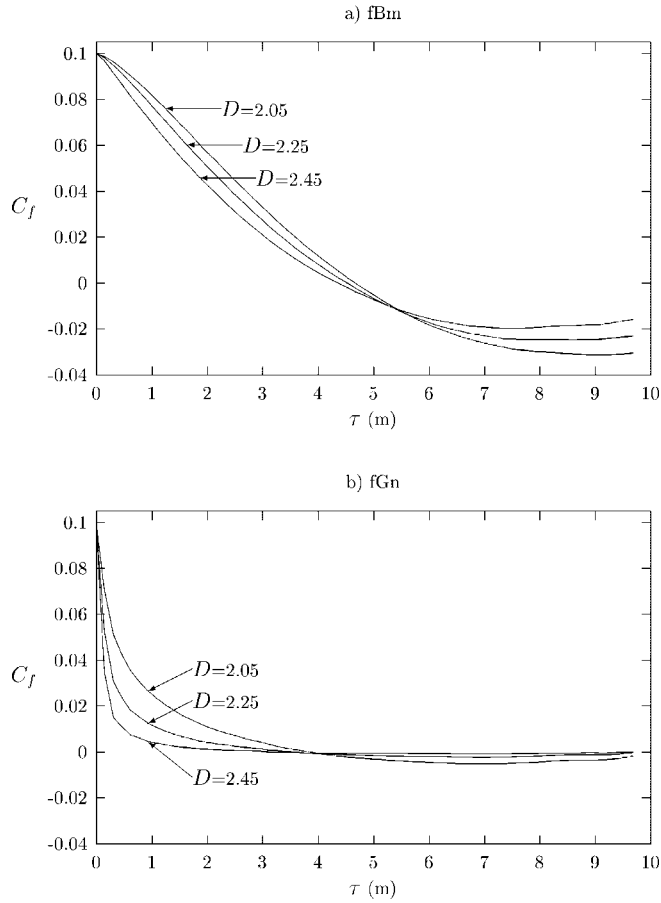

Figure 2. Covariance functions of fBm and fGn distributions for $D = 2.05$, 2.25, and 2.45.

Ω_k after N Monte Carlo realizations using the relations

$$\langle s_j \rangle^N = \langle s_j \rangle = \frac{1}{N} \sum_{m=1}^{N} s_j^m, \tag{12a}$$

$$\sigma_{s_j}^{2,N} = \frac{1}{N-1} \sum_{m=1}^{N} \left(s_j^m - \langle s_j \rangle \right)^2 = \frac{N}{N-1} \left[\langle (s_j)^2 \rangle - (\langle s_j \rangle)^2 \right], \tag{12b}$$

$$C_{s_j s_k}^N = \frac{1}{N} \sum_{m=1}^{N} (s_j - \langle s_j \rangle)(s_k - \langle s_k \rangle) = \langle s_j s_k \rangle - \langle s_j \rangle \langle s_k \rangle. \tag{12c}$$

Table 1. Parameters of the van Genuchten Model

	K_s (cm/s)	α_{vg} (cm^{-1})
$\langle F \rangle$	1.22×10^{-3}	0.075
σ_f^2	0.2	0.10

Note. n 1.89; θ_s 0.41; θ_r 0.065.

To illustrate the use of the Monte Carlo method and the performance of the hybridized mixed finite element procedure, we will consider the water flow in a rectangular domain Ω of 12 m in the horizontal direction by 8 m in the vertical direction. The water table is considered to be horizontal and located at a depth of 6 m. We consider a hydrostatic initial condition ($\mathbf{q} = 0$). At the upper boundary of Ω (surface, $z = 8$ m) we specify a constant infiltration rate of 12 mm/day over an interval of size 6 m at the center of this boundary. At the bottom ($z = 0$) and lateral boundaries of Ω we specified the values of the pressure head corresponding to the hydrostatic state. For the constitutive relations we use the van Genuchten model with parameter values corresponding to a sandy loam obtained by Carsel and Parrish (1988) and given in Table 1, where we also give the values for the variance of K_s and α_{vg} used for the generation of the corresponding fractal fields.

For the spatial discretization we employed a uniform mesh of 48×32 subdomains. The total simulation time for each realization was 15 days in order to develop an infiltration front in the upper part of the domain. The experiments were run on an IBM SP2 computer at Purdue University used as a single processor machine, with an average simulation time for each realization of 5 min. We ran a total of 1000 Monte Carlo simulations and then computed all statistical moments at $T = 15$ days as explained before.

Figures 3 and 4 display realizations of the fractal conductivity field K_s corresponding to the values in Table 1 for fBm and fGn distributions, respectively, and fractal dimension $D = 2.2$. The conductivity values show a high degree of heterogeneity, with an order of magnitude variation between minimum and maximum values. Also, as expected, we observe more persistence in the fBm than in the fGn realization of K_s.

In Figures 5 and 6 we show the water content θ at $T = 15$ days for a single realization of K_s and α_{vg} for fBm and fGn distributions and fractal dimension $D = 2.2$. In both cases it is clearly observed the effects of the local heterogeneities on the water content distribution in the soil.

Figures 7 and 8 display the corresponding flow fields for the same single realization, where we can observe the water motion where the infiltration is taking place (upper part of the domain), while in the rest of the domain the flow is negligible. In both figures the formation of preferential pathways by soil heterogeneities is clearly observed.

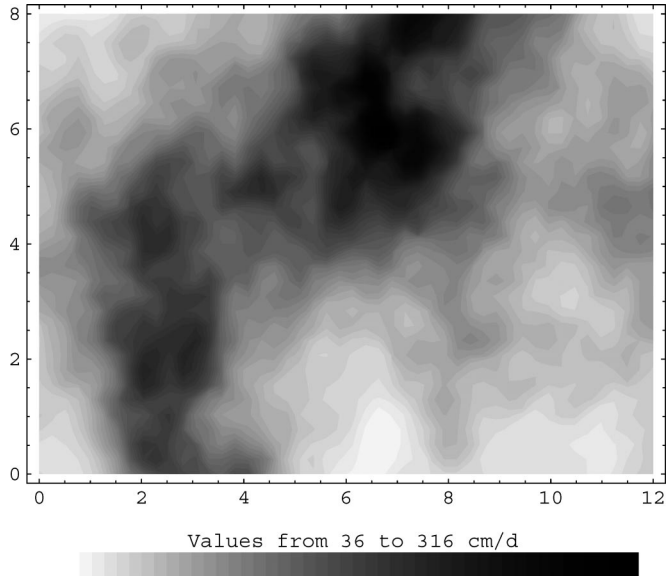

Figure 3. Realization of a permeability field K_s generated using fBm distributions.

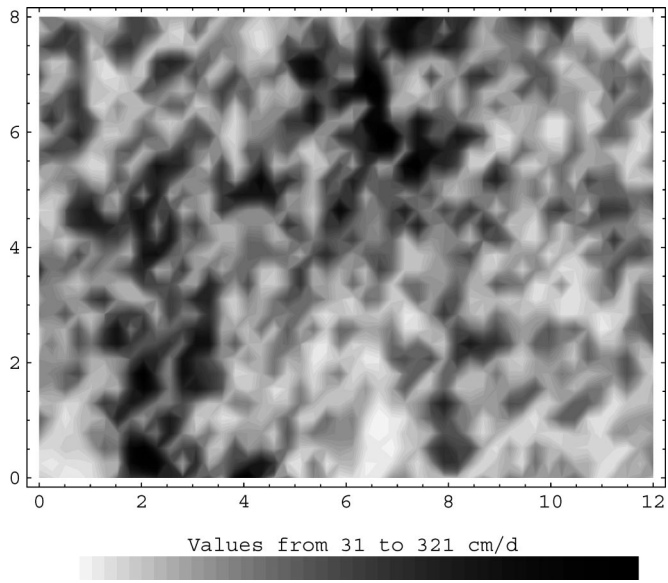

Figure 4. Realization of a permeability field K_s generated using fGn distributions.

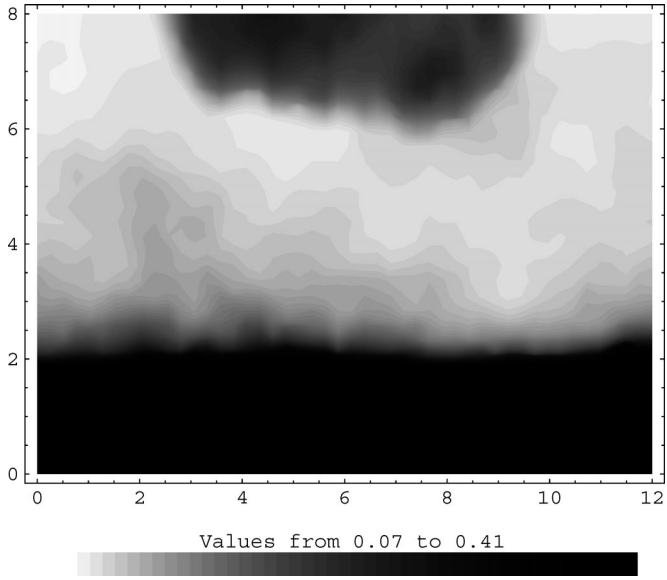

Figure 5. Realization of a water content field generated using fBm distributions.

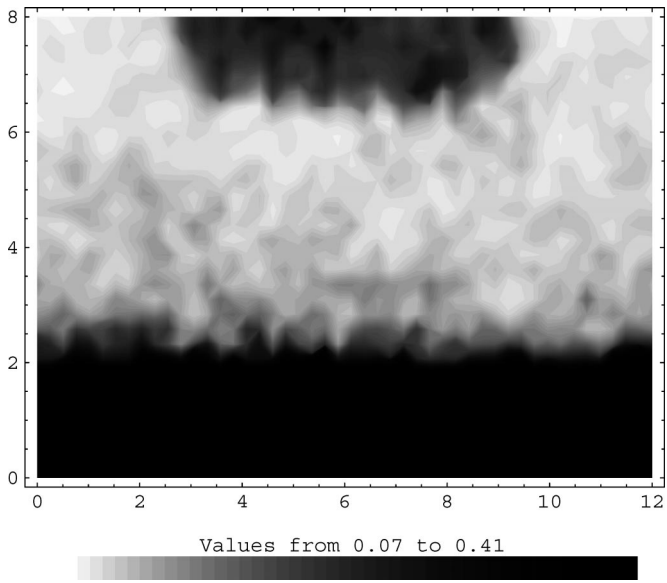

Figure 6. Realization of a water content field generated using fGn distributions.

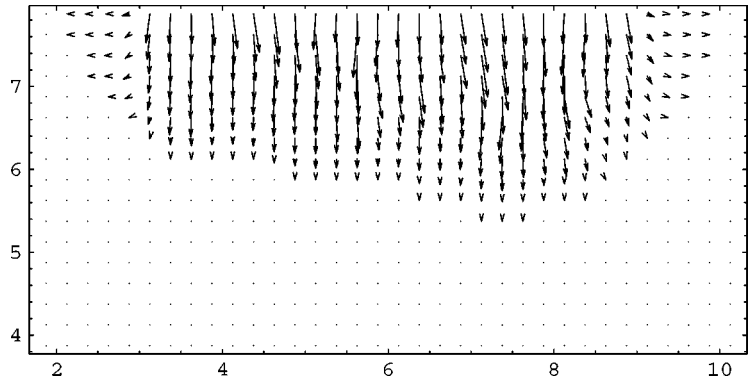

Figure 7. Realization of a water flow field generated using fBm distributions.

In Figures 9 and 10 we show the average and variance σ_θ^2 of the water content θ at $T = 15$ days for the case of an fBm distribution and fractal dimension $D = 2.2$. Notice that σ_θ^2 vanishes in the saturated zone since in this region $\theta(h) = \theta_s$. The variance σ_θ^2 attains its maximum values close to the water table, in the region known as the capillary fringe. This result shows the influence of the variability of soil parameters when studying variations in water table position. The variance σ_θ^2 also shows significative values along the infiltration front as is also mentioned by Ferrante and Yeh (1999).

Figures 11 and 12 display the average value and the variance of the vertical component q_z of the flow vector. It can be observed that the maximum values of the variance $\sigma_{q_z}^2$ are located in the region where the infiltration is taking place.

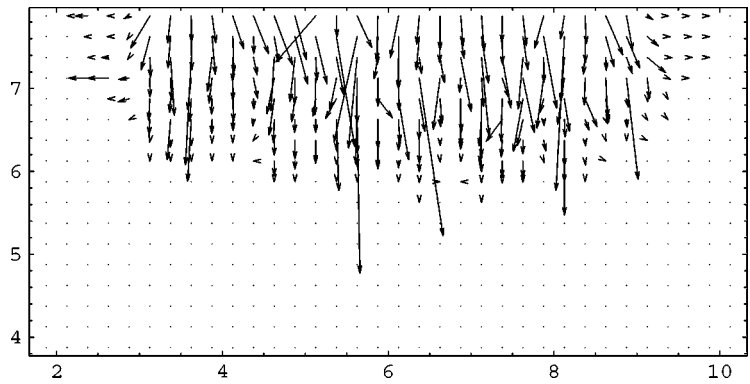

Figure 8. Realization of a water flow field generated using fGn distributions.

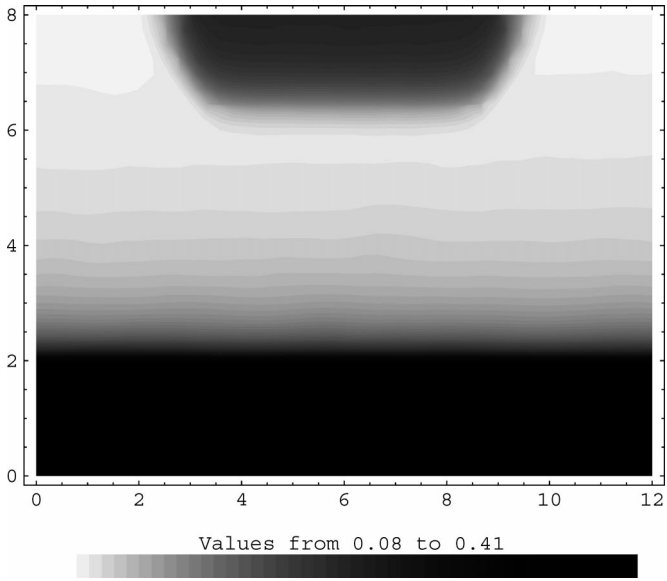

Figure 9. Mean water content field for fBm distributions and 1000 Monte Carlo realizations.

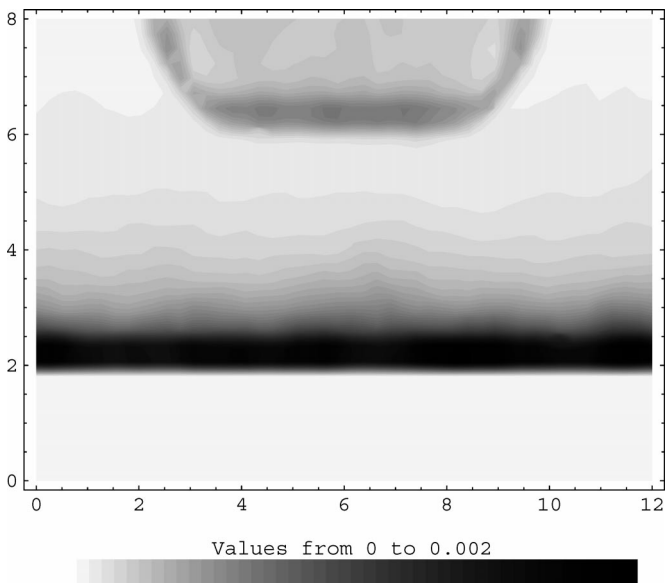

Figure 10. Variance of water content field for fBm distributions and 1000 Monte Carlo realizations.

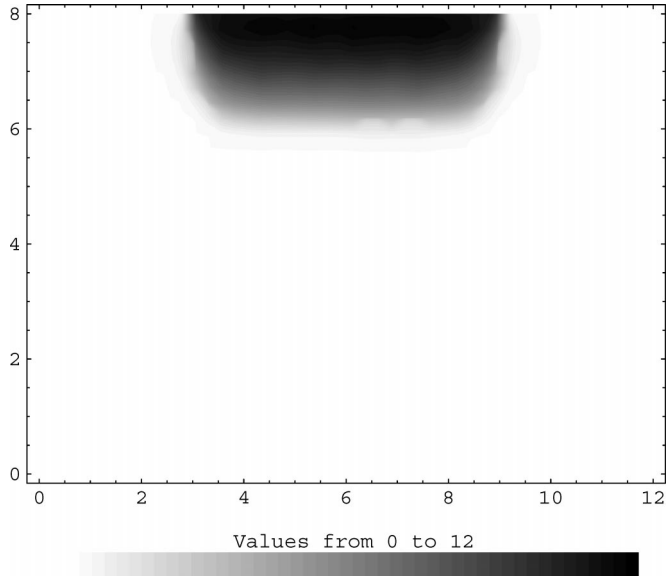

Figure 11. Mean q_z field for fBm distributions and 1000 Monte Carlo realizations.

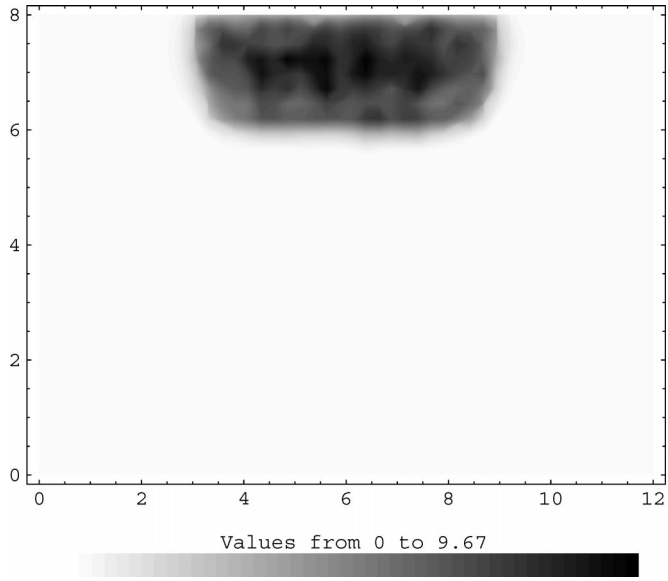

Figure 12. Variance of q_z for fBm distributions and 1000 Monte Carlo realizations.

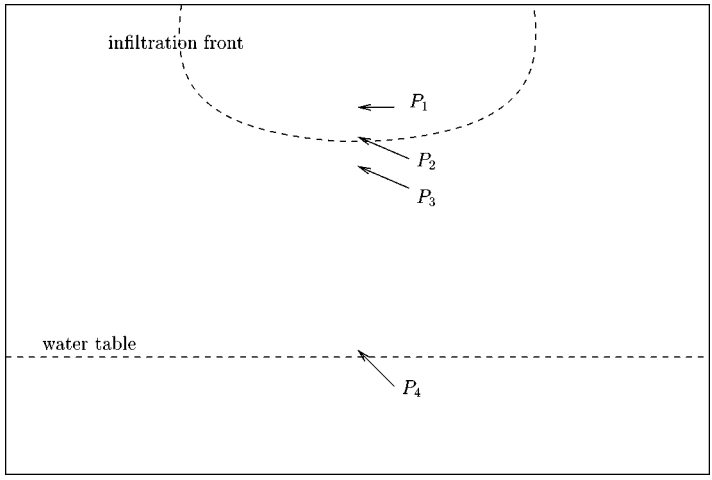

Figure 13. Position of the points P_i, $i = 1, \ldots, 4$ selected for the statistical analysis.

Next we present an experiment that illustrates the stabilization of the variance mentioned above. To show this behavior we selected, somewhat arbitrarily, four points as follows: $P_1 = (5.875, 6.625)$ in the infiltration region, $P_2 = (5.875, 6.125)$ approximately on the infiltration front, $P_3 = (5.875, 5.625)$ about 0.5 m below the infiltration front, and $P_4 = (5.875, 2.125)$ above the water table (Fig. 13). Figure 14 shows the variance σ_θ^2 of the water content assuming fBm distributions and $D = 2.2$ at time $T = 15$ days; it can be observed that the variance values stabilizes at the four points after 500 realizations. The same stabilization effect was observed for the other variables (h, q_x, q_z), for fGn distributions, and other fractal dimensions.

Next we analyze the behavior of the variance of the water content (σ_θ^2) for the case in which, for each realization of the stochastic permeability field K_s, the parameter α_{vg} is a random constant over the domain Ω with average value 0.075 cm^{-1} and variance of $\ln(\alpha_{vg})$ equal to 0.10. This simplification (that contradicts the experimental evidence presented by Russo and Bouton (1992) and Russo, Russo, and Laufer (1997)) is done by Tartakovsky, Neuman, and Lu (1999) to study stochastic unsaturated flow using a Kirchhoff transformation. Figure 15 shows values of σ_θ^2 at the point P_1 as a function of the number of Monte Carlo realizations for the case in which α_{vg} is either a constant over the domain Ω for each realization or a fBm process with $D = 2.2$. As expected, σ_θ^2 stabilizes much earlier in the former case. In particular, this figure shows that the numerical procedure is robust and capable to handle local heterogeneities in the parameter α_{vg}, used to represent local variability of the capillary relations in the unsaturated zone (c.f. (3)).

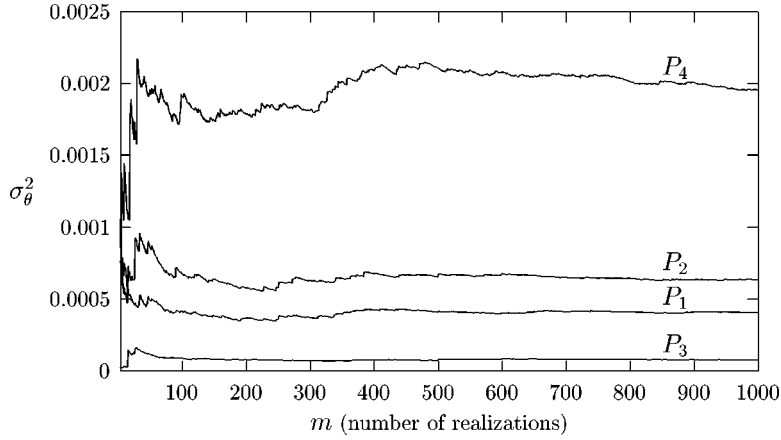

Figure 14. Stabilization of the water content variance at P_1, P_2, P_3, and P_4.

Figure 16 shows a log–log plot of the increments $\Delta\sigma_s^{2,m}$ as function of the number of realizations m for $s = \theta, h, q_x, q_z$. The figure shows that to obtain one order of magnitude in the error reduction in the calculation of the moments we need to increase in one order of magnitude the number of Monte Carlo realizations.

Finally, the covariance of the vertical component of the flow q_z in the horizontal and vertical directions is displayed in Figures 17 and 18, respectively, at the points P_1, P_2, and P_3. It can be observed that the covariances depend on the point and the direction at which are being calculated, showing numerically that the flow field is not stationary. Also note that in Figure 18 the covariance tends to zero

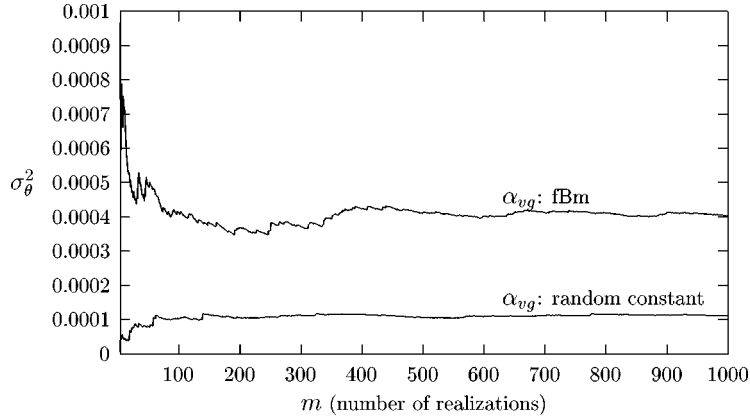

Figure 15. Influence of the parameter α_{vg} on the stabilization of the water content variance at P_1.

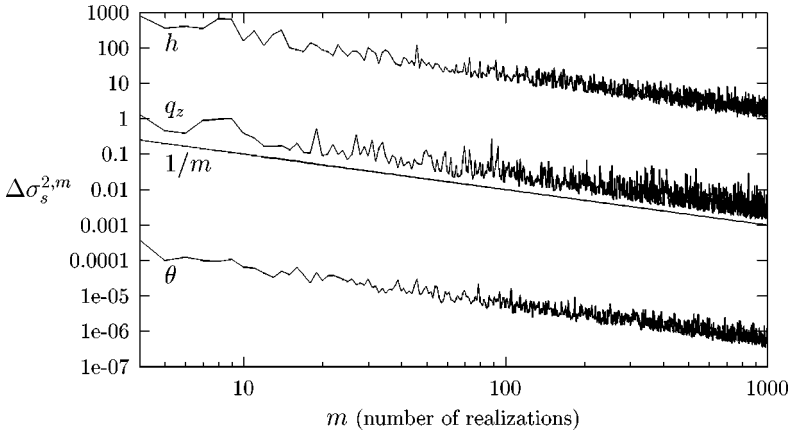

Figure 16. Convergence of the Monte Carlo simulation method.

near $z = 8$ m, i.e., close to the surface. This is due to the fact that the boundary condition imposed at such boundary is deterministic and of Neumann type; below the infiltration front the covariance also vanishes because the initial condition corresponds to the hydrostatic case ($\mathbf{q} = 0$). The covariance of the flow components are needed for the calculation of the macrodispersion coefficients (Dagan, 1989). This procedure is used by Lessoff, Idelman, and Dagan (2000) to study solute transport for steady state flow.

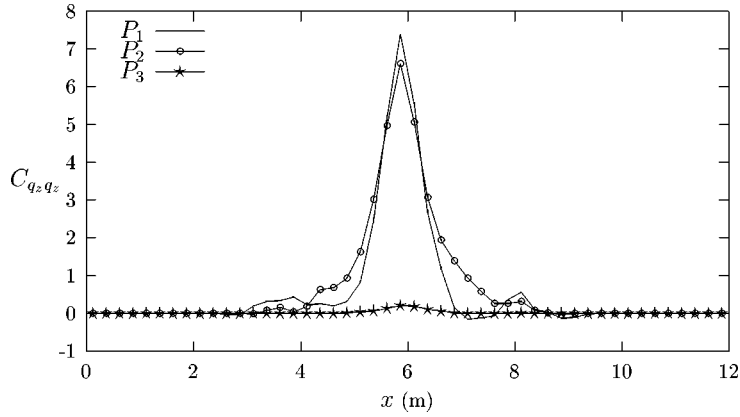

Figure 17. Covariance of q_z in the x-direction computed at the points P_1, P_2, and P_3.

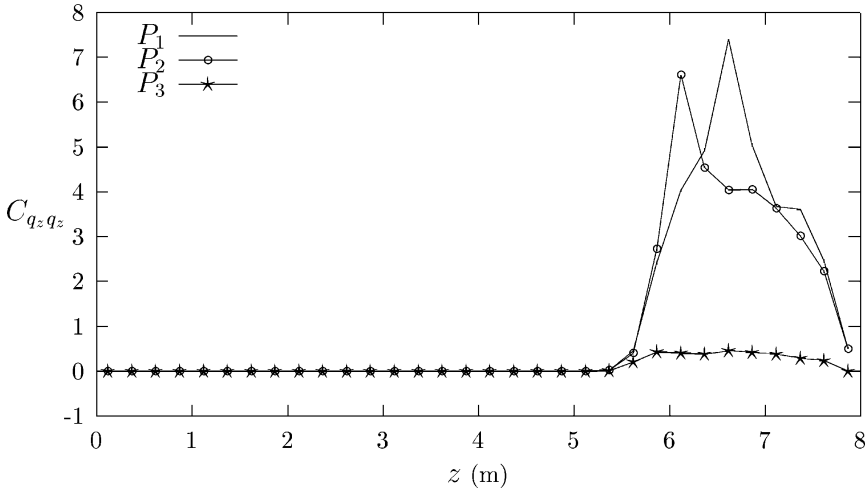

Figure 18. Covariance of q_z in the z-direction computed at the points P_1, P_2, and P_3.

CONCLUSIONS

A Monte Carlo simulation method for stochastic analysis of transient variably saturated flow is presented. Richards equation is solved employing a mixed finite element method. Hybridization of the mixed method provides a novel way to evaluate the hydraulic conductivity $K(h)$ on interelement boundaries by using Lagrange multipliers associated with the potential $h + z$.

A parametric analysis of the model was performed, analyzing the sensitivity of the dependent variables with respect to representative statistical parameters such as the fractal dimension and the distribution type (fBm/fGn) of the soil being modeled. The statistical moments of the water content, pressure head, and water flow were computed by averaging over realizations of the fractal parameters characterizing the soil heterogeneity. A new practical criteria to stop the Monte Carlo simulation based on the stabilization of the variances of the computed variables is also presented.

ACKNOWLEDGMENTS

This work has been funded in part by the Agencia Nacional de Promoción Científica y Tecnológica Argentina (contract BID 802/0C-AR) and CONICET, Argentina, PIP 0363/98. The authors wish to thank the Supercomputing Center at Purdue University for providing CPU time and technical advice.

REFERENCES

Allen, M. B., and Murphy, C., 1985, A finite element collocation method for variably saturated flows in porous media: Numer. Methods Partial Differ. Equations, v. 3, p. 229–239.

Arnold, D. N., and Brezzi, F., 1985, Mixed and nonconforming finitenelement methods: Implementation, postprocessing and error estimates: R.A.I.R.O. Modélisation, Mathématique et Analyse Numérique, v. 19, p. 7–32.

Beckie, R., Wood, E. F., and Aldama, A. A., 1993, Mixed finite element simulation of saturated groundwater flow using a multigrid accelerated domain decomposition technique: Water Resour. Res., v. 29, p. 3145–3157.

Bergamaschi, L., and Putti, M., 1999, Mixed finite elements and Newton-type linearization for the solution of Richards' equation: Int. J. Numer. Methods Eng., v. 45, p. 1025–1046.

Carsel, R. F., and Parrish, R. S., 1988, Developing join probability distributions of soil water characteristics: Water Resour. Res., v. 24, p. 755–769.

Celia, M. A., Bouloutas, E. T., and Zarba, R. L., 1990, A general mass-conservative numerical solution for the unsaturated flow equation: Water Resour. Res., v. 26, p. 1483–1496.

Chounet, L. M., Hilhorst, D., Jouron, C., Kelanemer, Y., and Nicolas, P., 1999, Simulation of water flow and heat transfer in soils by means of a mixed finite element method: Adv. Water Resour., v. 22, p. 445–460.

Dagan, G., 1989, Flow and transport in porous formations: Springer, New York, 465 p.

Douglas, J., Jr., and Roberts, J. E., 1985, Global estimates for mixed methods for second order elliptic equations: Math. Comput., v. 44, p. 39–52.

Ferrante, M., and Yeh, T. C. J., 1999, Head and flux variability in heterogeneous unsaturated soils under transient flow conditions: Water Resour. Res., v. 35, p. 1471–1479.

Guarracino, L., 2001, Modelado numérico del flujo de aguas subterráneas y transporte de solutos en medios porosos heterogéneos: Unpublished Doctoral Dissertation, Universidad Nacional de La Plata, Argentina, 118 p.

Harter, T., and Yeh, T. C. J., 1998, Flow in unsaturated random porous media, nonlinear numerical analysis and comparison to analytical stochastic models: Adv. Water Resour., v. 22, p. 257–272.

Hassan, A., Cushman, J. H., and Delleur, J. W., 1998, A Monte Carlo assessment of Eulerian flow and transport perturbation models: Water Resour. Res., v. 34, p. 1143–1163.

Kemblowski, M. W., and Chang, C. M., 1993, Infiltration in soils with fractal permeability distribution: Ground Water, v. 31, p. 187–192.

Lessoff, S. C., Idelman, P., and Dagan, G., 2000, A note on the influence of a constant velocity boundary condition on flow and transport in heterogeneous formations: Water Resour. Res., v. 36, p. 3095–3101.

Moltz, F. J., and Boman, G. K., 1995, Futher evidence of fractal structure in hydraulic conductivity distributions: Geophys. Res. Lett., v. 22, p. 2545–2548.

Moltz, F. J., Liu, H. H., and Szulga, J., 1997, Fractional Brownian motion and fractional Gaussian noise in subsurface hydrology: A review, presentation of fundamental properties and extensions: Water Resour. Res., v. 33, p. 2273–2286.

Mosé, R., Siegel, P., Ackerer, P., and Chavent, G., 1994, Application of the mixed hybrid finite element approximation in a groundwater flow model: Luxury or necessity?: Water Resour. Res., v. 30, p. 3001–3012.

Naff, R. L., Haley, D. F., and Sudicky, E. A., 1998, High-resolution Monte Carlo simulation of flow and conservative transport in heterogeneous porous media 1. Methodology and flow results: Water Resour. Res., v. 34, p. 663–677.

Nedelec, J., 1980, Mixed finite elements in R^3: Numer. Math., v. 35, p. 315–341.

Neuman, S. P., 1994, Generalized scaling of permeabilities: Validation and effect of support scale: Geophys. Res. Lett., v. 21, p. 349–352.

Raviart, P. A., and Thomas, J. M., 1977, A mixed finite element method for second order elliptic problems: Mathematical aspects of the finite element method: Lect. Notes Math., v. 606, p. 292–315.

Richards, L., 1931, Capillary conduction of liquids through porous mediums: Physics, v. 1, p. 318–333.

Ross, P. J., and Parlange, J. Y., 1994, Comparing exact and numerical solutions for Richards' equation for one-dimensional infiltration and drainage: Soil Sci., v. 157, p. 341–344.

Russo, D., and Bouton, M., 1992, Statistical analysis of spatial variability in unsaturated flow parameters: Water Resour. Res., v. 28, p. 1911–1925.

Russo, D., Russo, I., and Laufer, A., 1997, On the spatial variability of parameters of the unsaturated hydraulic conductivity: Water Resour. Res., v. 33, p. 945–956.

Salandin, P., and Fiorotto, V., 1998, Solute transport in highly heterogeneous aquifers: Water Resour. Res., v. 34, p. 949–961.

Strivastava, R., and Yeh, T. C. J., 1991, Analytical solutions for one-dimensional, transient infiltration toward the water table in homogeneous and layered soils: Water Resour. Res., v. 27, p. 753–762.

Tartakovsky, D. M., Neuman, S. P., and Lu, Z., 1999, Conditional stochastic averaging of steady state unsaturated flow by means of Kirchhoff transformation: Water Resour. Res., v. 35, p. 731–745.

Ünlü, K., Nielsen, D. R., and Biggar, J. W., 1990, Stochastic analysis of unsaturated flow: One-dimensional Monte Carlo simulation and comparisons with spectral perturbation analysis and field observations: Water Resour. Res., v. 26, p. 2207–2218.

van Genutchen, M. T., 1980, A closed-form equation for predicting the hydraulic conductivity of unsaturated soils: Soil Sci. Soc. Am. J., v. 44, p. 892–898.

Voss, R. F., 1988, Fractals in nature: From characterization to simulation, *in* Peitgen, H., and Saupe, D., eds., The science of fractal images: Springer, New York, p. 21–69.